THE JOURNAL OF PHYSICAL CHEMISTRY A

Article

Cite This: J. Phys. Chem. A 2018, 122, 601−609

pubs.acs.org/JPCA

Generation and Stability of the *gem*-Diol Forms in Imidazole Derivatives Containing Carbonyl Groups. Solid-State NMR and Single-Crystal X-ray Diffraction Studies

Ayelén Florencia Crespi,[†] Agustín Jesús Byrne,[†] Daniel Vega,[‡] Ana Karina Chattah,[§] Gustavo Alberto Monti,[§] and Juan Manuel Lázaro-Martínez*[,†,∥]

[†]Facultad de Farmacia y Bioquímica, Departamento de Química Orgánica, Universidad de Buenos Aires, Junín 956 (C1113AAD), CABA, Argentina

[‡]Departamento de Física de la Materia Condensada, Comisión Nacional de Energía Atómica, Av. Gral. Paz 1499 (1650) San Martín, Buenos Aires, Argentina

[§]FaMAF & IFEG-CONICET, Universidad Nacional de Córdoba, Medina Allende s/n (X5000HUA), Córdoba, Argentina

[∥]IQUIFIB-CONICET, Junín 956 (C1113AAD), CABA, Argentina

Supporting Information

ABSTRACT: The stability of *gem*-diol forms in imidazolecarboxaldehyde isomers was studied by solid-state nuclear magnetic resonance (ss-NMR) combined with single-crystal X-ray diffraction studies. These methodologies also allowed determining the factors governing the occurrence of such rare functionalization in carbonyl moieties. Results indicated that the position of the carbonyl group is the main factor that governs the generation of geminal diols, having a clear and direct effect on hydration, since, under the same experimental conditions, only 36% of 5-imidazolecarboxaldehydes and 5% of 4-imidazolecarboxaldehydes were hydrated, as compared to 2-imidazolecarboxaldehydes, with which a 100% hydration was achieved. Not only did trifluoroacetic acid favor the addition of water to the carbonyl group but also it allowed obtaining single crystals. Single crystals of the *gem*-diol and the hemiacetal forms 2-imidazolecarboxaldehyde and *N*-methyl-2-imidazolecarboxaldehyde, respectively, were isolated and studied through ^{1}H ss-NMR. Mass spectrometry and solution-state NMR experiments were also performed to study the hydration process.

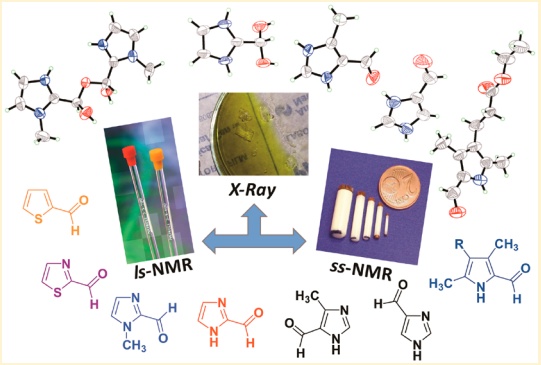

1. INTRODUCTION

Understanding the chemistry of *gem*-diols is crucial for the development of synthetic methods to obtain new organic ligands, which are often used for the design of single-molecule magnets and metal complexes.[1−8] A high number of metal complexes bearing *gem*-diols has been reported,[4−16] in which the presence of these moieties is generally demonstrated by single-crystal X-ray diffraction.[17−20] As a rule, the stability of this functional group is not studied in the free ligand before the preparation of the metal complex.

Among the wide variety of heterocyclic aldehydes used as chelating ligands, the imidazolecarboxaldehyde isomers[21−27] and pyridinecarboxaldehyde compounds[7−10,13,14,28,29] are relevant due to their potential capacity to remove toxic metals from the body.[21] In this context, we previously reported the isolation of the neutral *gem*-diol form of the 2-imidazolecarboxaldehyde in the solid state.[20] This compound, together with the hydrated form of 4-pyridinecarboxaldehyde[11] and related compounds (Scheme 1),[19] was the first *gem*-diol form to be reported for aromatic heterocyclic molecules. Particularly, the *gem*-diol form of 2-imidazolecarboxaldehyde cannot be obtained with water but by the addition of 95:5 (v/v) H_2O/trifluoroacetic acid (TFA; Scheme 1).[19]

As for biochemistry aspects, solution-state NMR and X-ray crystallography experiments have been used to confirm the formation of *gem*-diol and hemiacetal structures, for example, as intermediate structures in the binding of α-chymotrypsin with a macrocyclic peptidomimetic aldehyde.[17] Particularly, X-ray studies have been conducted to elucidate the structure of a *gem*-diol intermediate in the catalysis exerted by the HIV-1 protease.[30,31] Furthermore, solid-state NMR (ss-NMR) is a useful methodology to elucidate the chemical composition of mixtures in which both *gem*-diol and carbonyl forms are present.[19] In the latter cases, on the one hand, high-performance liquid chromatography techniques may be used; however, dissolution of the sample in acid/water mixtures and proper optimization of the chromatographic system are

Received: December 16, 2017
Published: December 20, 2017

DOI: 10.1021/acs.jpca.7b12390
J. Phys. Chem. A 2018, 122, 601−609

Scheme 1. Previous NMR Hydration Studies[a]

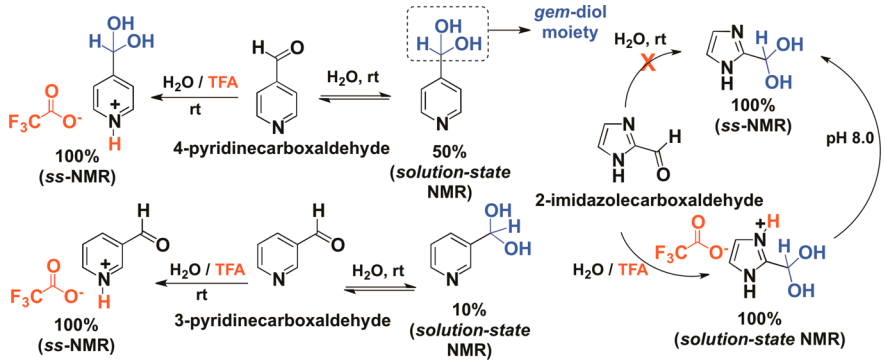

[a]Performed in pyridinecarboxaldehyde and 2-imidazolecarboxaldehyde compounds.

required. On the other hand, solution-state NMR studies can be easily performed and analyzed in a broad variety of solvents (D_2O, D_2O/NaOD, CD_3OD, deuterated dimethyl sulfoxide (DMSO-d_6), D_2O/TFA, among others).

To have an insight into the chemistry of *gem*-diol compounds, the aim of this work was to study the *gem*-diol generation in imidazolecarboxaldehydes through the combination of ss-NMR and single-crystal X-ray diffraction techniques. Complementary analyses were performed by solution-state NMR, high-resolution mass spectrometry (HRMS), and ^{1}H ss-NMR.

2. EXPERIMENTAL SECTION

2.1. Synthesis. TFA (99%), 4-pyridinecarboxaldehyde ($\mathbf{P_1}$, 97%), 4-methylthiazole-2-carboxaldehyde ($\mathbf{T_1}$, 97%), 2-thiophenecarboxaldehyde ($\mathbf{T_2}$, 98%), 1-methyl-2-imidazolecarboxaldehyde ($\mathbf{A_2}$, 98%), 4-methyl-5-imidazolecarboxaldehyde ($\mathbf{A_3}$, 99%), 4-imidazolecarboxaldehyde ($\mathbf{A_4}$, 98%), deuterium oxide (D_2O, 99.9 atom %D), DMSO-d_6, (99.96 atom %D), and methanol-d_4 (CD_3OD, >99.8 atom %D) were purchased from commercial sources and were used without further purification. The 2-imidazolecarboxaldehyde ($\mathbf{A_1}$)[20] and ethyl 3-(5-formyl-2,4-dimethyl-1*H*-pyrrol-3-yl)propanoate ($\mathbf{P_2}$) compounds were synthesized according to previous reports.[32]

The general quantitative synthesis of the corresponding neutral *gem*-diol solid forms for 2-imidazolecarboxaldehyde $\mathbf{A_1}$ ($\mathbf{H_1}$) and 4-pyridinecarboxaldehyde $\mathbf{P_1}$ ($\mathbf{P_{1H}}$) were performed as described elsewhere.[19,20] Solid imidazolium-trifluoroacetate derivatives containing both *gem*-diol and hemiacetal ($\mathbf{H_n}$**.TFA** and $\mathbf{HA_n}$**.TFA**), carbonyl, and carboxylic acid moieties ($\mathbf{A_n}$**.TFA** and $\mathbf{CA_n}$**.TFA**) were prepared by incubation of 50 mmol of $\mathbf{A_n}$ in 3 mL of 95:5 (v/v) TFA/H_2O for 24 h at room temperature. Solutions were then lyophilized and stored in a desiccator until NMR measurements were performed.

2.2. NMR Experiments. High-resolution ^{13}C solid-state spectra for the different compounds were recorded using the ramp ^{1}H−^{13}C cross-polarization and magic angle spinning (CP-MAS) sequence with proton decoupling during acquisition. The ^{13}C CP-MAS experiments were performed at room temperature in a Bruker Avance-II 300 spectrometer equipped with a 4 mm MAS probe. The operating frequency for protons and carbons was 300.13 and 75.46 MHz, respectively. Glycine was used as an external reference for the ^{13}C spectra and to set the Hartmann−Hahn matching condition in the cross-polarization experiments in ^{13}C spectra. The recycling time was 4 s. The contact time during CP was 1500 μs for ^{13}C spectra. The small-phase incremental alternation with 64 steps (SPINAL64) sequence was used for heteronuclear decoupling during acquisition with a proton field H_{1H} satisfying $\omega_{1H}/2\pi = \gamma_H H_{1H} = 62$ kHz.[33] The spinning rate for all the samples was 10 kHz. Different contact times were used (1.0−2.0 ms) to obtain a compromise between the signal-to-noise ratio in each scan and the total time of the experiments, with number of scans between 2000 and 4000. The two-dimensional (2D) ^{1}H−^{13}C HETCOR experiment in the solid state was recorded following the sequence presented by van Rossum et al.[34] The contact time for the CP was 150 μs to avoid relayed homonuclear spin-diffusion-type processes. The magic angle pulse length was 2.55 μs. To obtain the ^{1}H spectra, 64 points were collected with a dwell time of 35.5 μs. The acquisition time was 1.14 ms, and the spinning rate was 10 kHz. The ^{1}H MAS experiments were performed in a Bruker Ascend-600 spectrometer equipped with a 2.5 mm MAS probe with an operating frequency for protons of 600.09 MHz. ^{1}H chemical shifts were indirectly referenced relative to neat tetramethylsilane using powdered glycine as an external reference.

The solution-state NMR experiments were performed at room temperature in a Bruker Avance-II 300 or Bruker Ascend-600 spectrometer. To determine the hydration of the carbonyl group, ∼30 mg of each compound was dissolved in D_2O or 95:5 (v/v) D_2O/TFA.

2.3. Single-Crystal X-ray Studies. Single-crystals were grown and isolated by slow evaporation of the solvent at room temperature from each solution, in which the solid compound was dissolved as indicated in Section 2.1 without the lyophilization step. Single-crystal X-ray diffraction data were collected at room temperature, using a Gemini A diffractometer, Oxford Diffraction, Eos CCD detector with graphite-monochromated Mo Kα (λ = 0.710 73 Å) radiation. Data-collection strategy and data reduction followed standard procedures implemented in the CrystAlisPro software. Different reflections were collected for each sample, and they are specified in the Supporting Information section. The structures were solved using SHELXS-97 program[35] and refined using the full-matrix LS procedure with SHELXL-2014/7.[36] Anisotropic displacement parameters were employed for non-hydrogen atoms. All hydrogen atoms were located at the expected positions, and they were refined using a riding model.

2.4. HRMS Studies. The HRMS results were recorded in a Bruker micrOTOF-Q II spectrometer equipped with an electrospray ionization (ESI). The solid samples were dissolved in 50:50 (v/v) water/methanol or 20:60:20 (v/v) water/

DOI: 10.1021/acs.jpca.7b12390
J. Phys. Chem. A 2018, 122, 601−609

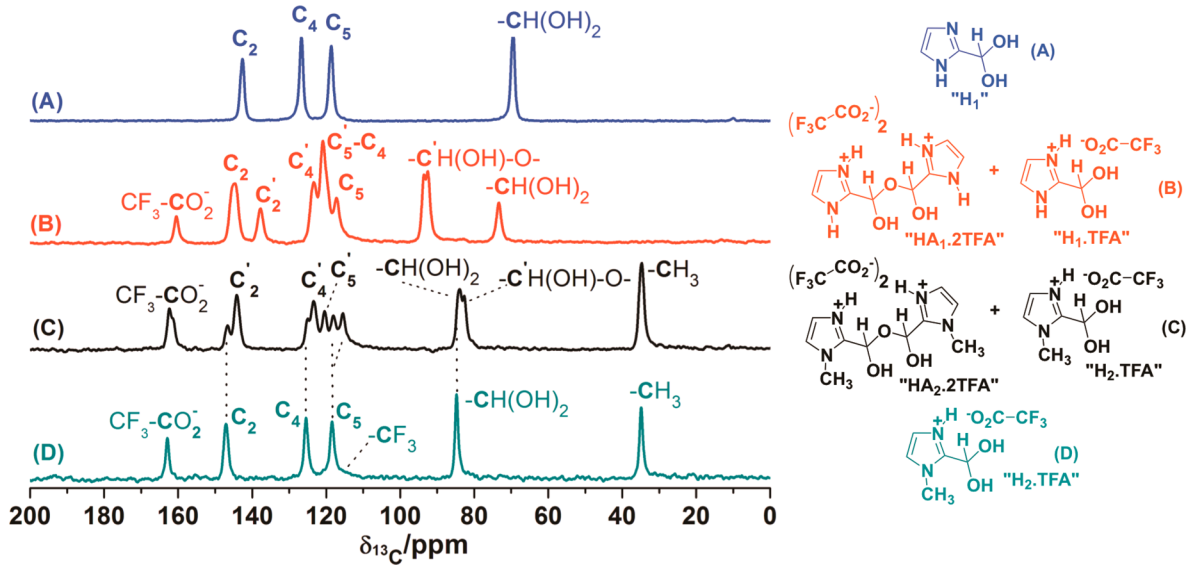

Figure 1. ^{13}C CP-MAS spectra corresponding to the *gem*-diol form of the 2-imidazolecarboxaldehyde $\mathbf{A_1}$ ($\mathbf{H_1}$); the remaining solids obtained after the evaporation of the solvents in a $\mathbf{A_1}$ (B) or $\mathbf{A_2}$ (C) 95:5 (v/v) TFA/H_2O solutions and the *gem*-diol form of *N*-methyl-2-imidazolecarboxaldehyde obtained from the sample in spectrum C dissolved in water and lyophilized (D). For the hemiacetal structures in spectra B and C, the assignment is indicated with an apostrophe.

methanol/DMSO prior to the ESI HRMS determination in positive mode.

3. RESULTS AND DISCUSSION

3.1. Hydration Studies in 2-Imidazolecarboxaldehydes by ^{13}C CP-MAS Solid-State NMR. The *gem*-diol form of 2-imidazolecarboxaldehyde $\mathbf{A_1}$ ($\mathbf{H_1}$) was first studied by ss-NMR (Figure 1). The ^{13}C CP-MAS spectrum of the neutral *gem*-diol form of $\mathbf{A_1}$ ($\mathbf{H_1}$) presented a signal at δ^{13}C = 69.6 ppm (-CH(OH)$_2$), while the signal corresponding to the carbonyl group at δ^{13}C = 180.4 ppm (-CHO)[20] in $\mathbf{A_1}$ was not observed, which indicates that only the *gem*-diol derivative was present (Figure 1A).

The fact that the ^{1}H NMR spectrum corresponding to $\mathbf{A_1}$ dissolved in 95:5 (v/v) D_2O/TFA indicated that 100% of the chemical entities corresponded to the *gem*-diol form (Table 1)

Table 1. Amount of *gem*-Diol and Aldehyde Forms for the Indicated Carbonyl Compounds As Determined by ^{1}H NMR

	^{1}H NMR			
	D_2O		95:5 (v/v) D_2O/TFA	
compound	*gem*-diol	aldehyde	*gem*-diol	aldehyde
2-imidazolecarboxaldehyde ($\mathbf{A_1}$)		100	100	
N-CH_3-2-imidazolecarboxaldehyde ($\mathbf{A_2}$)		100	100	
4-CH_3-5-imidazolecarboxaldehyde ($\mathbf{A_3}$)		100	5	95
4-imidazolecarboxaldehyde ($\mathbf{A_4}$)		100	36	64
2-CHO-4-CH_3-thiazole ($\mathbf{T_1}$)	*a*	*a*	100	
2-CHO-thiophene ($\mathbf{T_2}$)	*a*	*a*		100
4-pyridinecarboxaldehyde ($\mathbf{P_1}$)[19]	50	50	100	
2-CHO-3,5-(CH_3)$_2$-4-PEt-pyrrole ($\mathbf{P_2}$)[b]	*a*	*a*		100

[a]Insoluble in water. [b]Ethyl 3-(5-formyl-2,4-dimethyl-1*H*-pyrrol-3-yl)propanoate.

prompted us to obtain TFA-salt crystals. X-ray studies of single crystals obtained for $\mathbf{A_1}$ in 95:5 (v/v) TFA/H_2O allowed elucidating the chemical structure of $\mathbf{H_1.TFA}$, in which the *gem*-diol moiety is present (Figure 2 and Supporting Information). However, the analysis of the solid remaining after the complete evaporation of the solvent revealed the presence of the hydrate form (δ^{13}C = 73.2 ppm, -CH(OH)$_2$) together with a hemiacetal form ($\mathbf{HA_1}$) (δ^{13}C = 92.4 ppm, -CH(OH)-O−; Figure 1B and Scheme S1). On the one hand, the ^{1}H NMR spectrum, obtained in DMSO-d_6, of the crystalline sample studied in Figure 1B showed that the hemiacetal ($\mathbf{HA_1}$, δ^1H = 6.51 ppm, -CH(OH)-O−), carbonyl ($\mathbf{A_1}$, δ^1H = 9.66 ppm, -CHO) and *gem*-diol ($\mathbf{H_1}$, δ^1H = 6.06 ppm, -CH(OH)$_2$) forms were present in 42%, 42%, and 16%, respectively (Figure S1 and Scheme S1). On the other hand, the same sample dissolved in D_2O only led to the *gem*-diol form with a proton chemical shift of 6.12 ppm (Figure S2). These results indicated that ^{13}C CP-MAS NMR is the best technique for identifying *gem*-diols by observing the range of 70−100 ppm.

As for *N*-methyl-2-imidazolecarboxaldehyde ($\mathbf{A_2}$), preliminary ^{1}H solution-state NMR studies have shown that, in the absence of TFA, the hydration of the carbonyl group could not be achieved (Figure S4). In contrast, the hydration was quantitative in the presence of TFA (Table 1 and Figure S5). In consequence, single crystals for $\mathbf{A_2}$ were obtained when 95:5 (v/v) TFA/H_2O was employed, which indicated the presence of the hemiacetal form ($\mathbf{HA_2.2TFA}$; Figure 2). Not only did the ^{13}C CP-MAS spectrum of the solid remaining after the evaporation of solvents show the hemiacetal $\mathbf{HA_2.2TFA}$ form but also it demonstrated the presence of the *gem*-diol form of $\mathbf{A_2}$ ($\mathbf{H_2.TFA}$; Figure 1C). Particularly, the hydrate and the hemiacetal forms of $\mathbf{A_2}$ presented the same ^{13}C chemical shift signals (~83 ppm, Figure 1C). Conversely, a difference of 20 ppm was observed between the *gem*-diol ($\mathbf{H_1}$, 73.1 ppm) and the hemiacetal ($\mathbf{HA_1}$, ~93 ppm) forms of $\mathbf{A_1}$ (Figure 1B).

The solid whose spectrum is depicted in Figure 1C was dissolved in D_2O and analyzed by ^{1}H NMR, to show that only the *gem*-diol form $\mathbf{H_2}$ was present (Figure S6). However, when

DOI: 10.1021/acs.jpca.7b12390
J. Phys. Chem. A 2018, 122, 601−609

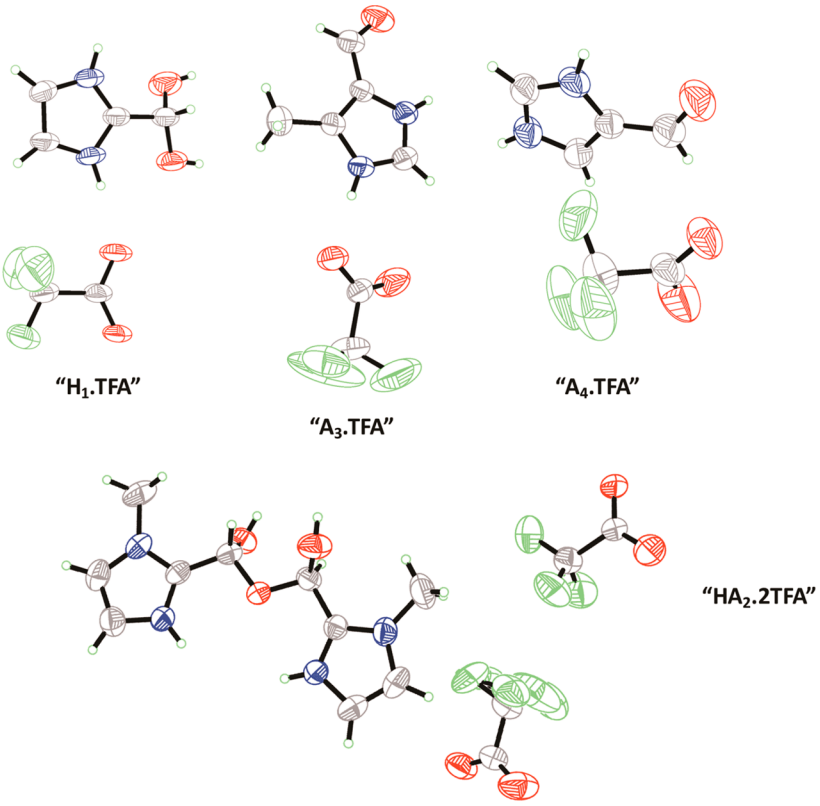

Figure 2. Crystal structures for $\mathbf{H_1}$**.TFA**, $\mathbf{A_3}$**.TFA**, $\mathbf{A_4}$**.TFA**, and $\mathbf{HA_2}$**.2TFA**. The displacement ellipsoids for the non-H atoms in the figure were drawn at the 50% probability level.

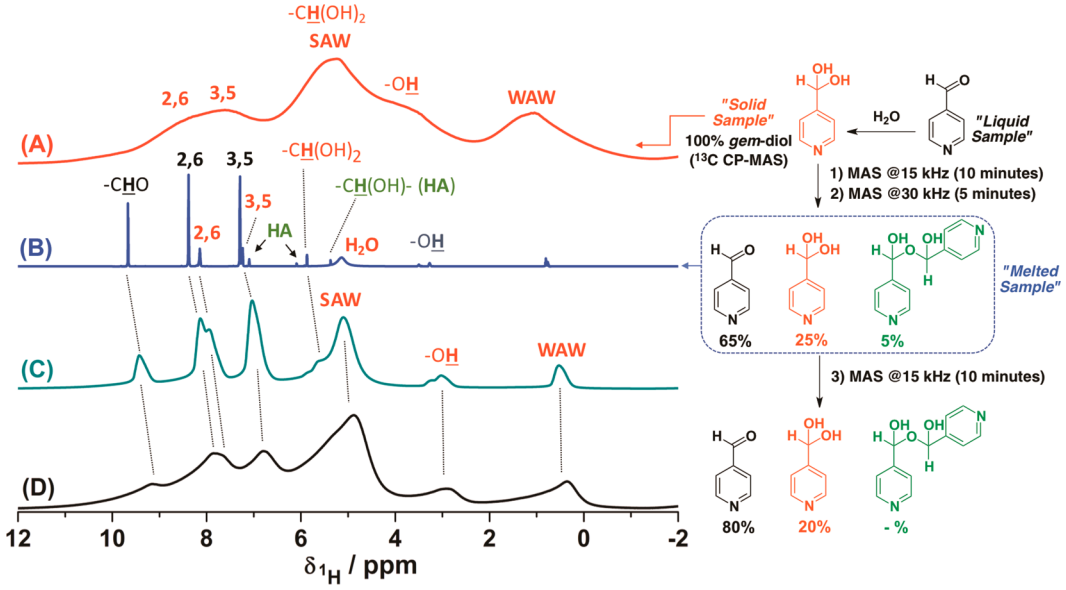

Figure 3. ^{1}H MAS NMR spectra corresponding to a solid *gem*-diol form of 4-pyridinecarboxaldehyde at a MAS rate of 15 (A) and 30 (B) kHz and the reduction to the initial MAS rates of 15 (C) and 5 (D) kHz.

the same solid was dissolved in DMSO-d_6, the ^{1}H NMR spectrum displayed both the carbonyl ($\mathbf{A_2}$, δ^1H = 9.71 ppm, -C**H**O) and *gem*-diol ($\mathbf{H_2}$, δ^1H = 6.14 ppm, -C**H**$(OH)_2$) signals (Figure S7 and Scheme S1). Unfortunately, all the single-crystal samples obtained corresponded to the hemiacetal structure $\mathbf{HA_2}$ and not to the *gem*-diol form ($\mathbf{H_2}$). The signals obtained in the ^{13}C CP-MAS spectrum of the solid obtained after the lyophilization of the aqueous solution containing the trifluoroacetates $\mathbf{H_2}$**.TFA/**$\mathbf{HA_2}$**.2TFA** corresponded to the *gem*-diol form ($\mathbf{H_2}$, δ^{13}C = 84.9 ppm, -$CH(OH)_2$). This assignment allowed the unequivocal identification of the carbon resonance signals in the spectrum of Figure 1C, where $\mathbf{H_2}$ and $\mathbf{HA_2}$ (δ^{13}C = 83.2 ppm, -CH(OH)-O−) were present. Regarding the solid sample containing both $\mathbf{H_1}$**.TFA** and $\mathbf{HA_1}$**.2TFA** (Figure 1B), the nonequivalence of the hemiacetal carbons at ∼94 ppm may be associated with either an

DOI: 10.1021/acs.jpca.7b12390
J. Phys. Chem. A 2018, 122, 601−609

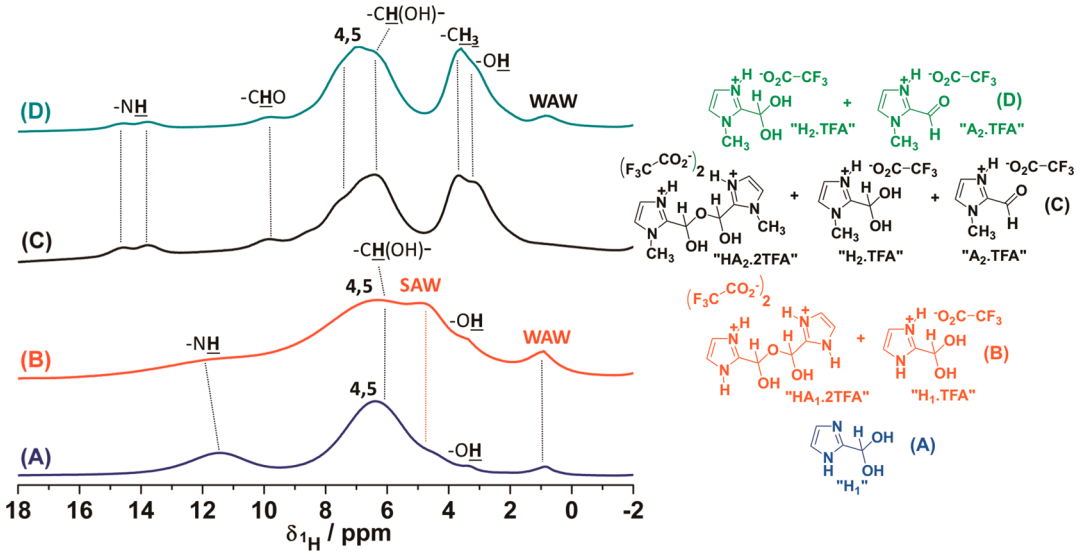

Figure 4. ^{1}H MAS NMR (30 kHz) spectra corresponding to *gem*-diol form of the 2-imidazolecarboxaldehyde (A), crystals obtained from a 2-imidazolecarboxaldehyde 95:5 (v/v) TFA/H_2O solution (B) or a *N*-methyl-2-imidazolecarboxaldehyde 95:5 (v/v) TFA/H_2O solution (C), and the *gem*-diol form of *N*-methyl-2-imidazolecarboxaldehyde (D). The chemical composition was obtained from the ^{13}C CP-MAS spectra (Figure 1) and the ^{1}H MAS NMR spectra of this figure.

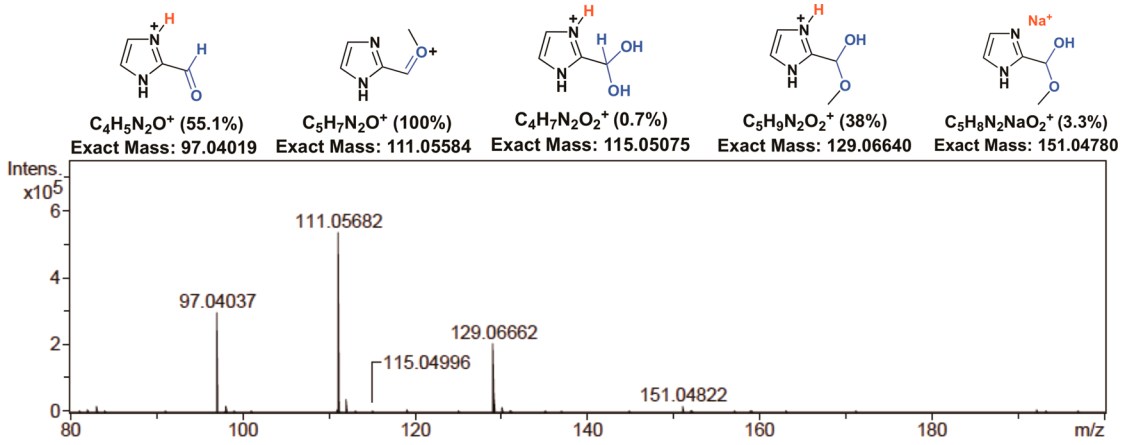

Figure 5. HRMS spectrum for the solid studied by ss-NMR in spectra B (Figure 1) dissolved in 50:50 (v/v) methanol/water.

asymmetry present in the molecule or with the presence of more than one molecule per unit cell, since the treatment with water only affects the relative content of each molecule in terms of the *gem*-diol and hemiacetal forms (C_2, Figure 1B and Scheme S1).

3.2. Hydration Studies in Imidazole-2-carboxaldehydes and 4-Pyridinecarboxaldehyde by ^{1}H-MAS ss-NMR. To explore the hydration process in molecules bearing carbonyl groups, ^{1}H ss-NMR spectra at different MAS rates were obtained. Results for the hydrated form of 4-pyridinecarboxaldehyde $\mathbf{P_1}$ are shown in Figure 3. Proton resonance signals were tentatively assigned according to previous hydration NMR results for the *gem*-diol forms of 4-pyridinecarboxaldehyde and 3-chloro-4-pyridinecarboxaldehyde in DMSO-d_6 and D_2O.[19] At a MAS rate of 15 kHz, the spectrum displayed broad signals that would correspond to the *gem*-diol form of $\mathbf{P_1}$ ($\mathbf{P_{1H}}$; Figure 3A), since the ^{13}C CP-MAS (at 10 kHz MAS) only revealed the presence of the *gem*-diol form.[19] Interestingly, the ^{1}H MAS NMR spectrum displayed different water environments, which might be related to the presence of strongly associated water (SAW, δ^1H = 5.3 ppm) and weakly associated water (WAW, δ^1H = 1.0 ppm).[37,38] However, when the MAS rate was increased to 30 kHz to enhance the resolution of the proton line (Figure 3B), and according to the line integration, 65% of the *gem*-diol form reverted to the parent aldehyde. Under these experimental conditions, the hemiacetal structure was also present in 5%, as indicated by "**HA**" in Figure 3B. This fact is indicative that, at a MAS rate of 30 kHz, the sample melted inside the rotor (mp 70−72 °C) with the consequent loss of water, which was inferred by the proton aldehyde signal at δ^1H = 9.7 ppm, giving rise to a spectrum that is similar to that obtained when a solution-state ^{1}H NMR is performed. When the MAS rate was reduced to 15−5 kHz, the broadening of the NMR lines was observed again due to the solidification of the *gem*-diol inside the rotor (Figure 3C,D). In addition, the water domains (SAW and WAW) were recovered together with the proton of the hydroxyl groups. It is noteworthy that the solid sample inside the rotor did not recover its initial composition after the MAS rate reduction (Figure 3D).

The same experiments were performed for the solid samples containing $\mathbf{H_1}$, $\mathbf{H_1}$**.TFA/**$\mathbf{HA_1}$**.2TFA**, $\mathbf{H_2}$**.TFA**, and $\mathbf{H_2}$**.TFA/**

DOI: 10.1021/acs.jpca.7b12390
J. Phys. Chem. A 2018, 122, 601−609

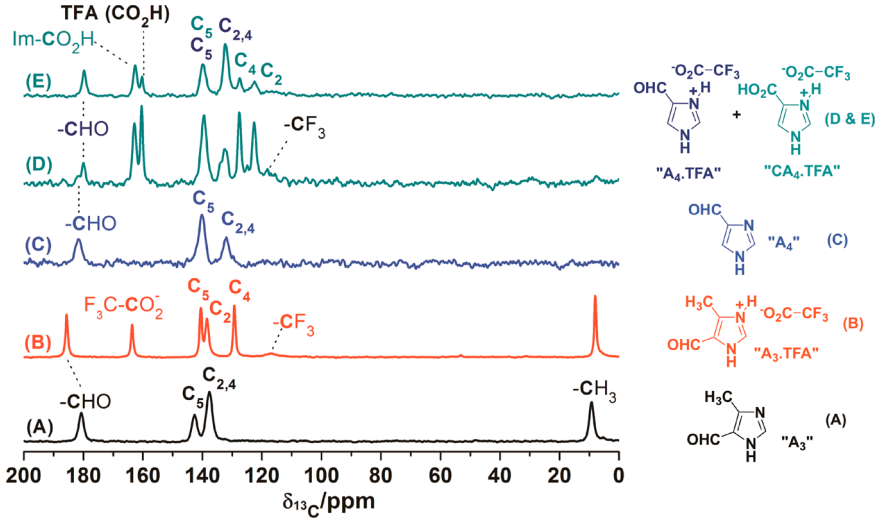

Figure 6. ^{13}C CP-MAS spectra corresponding to 4-methyl-5-imidazolecarboxaldehyde $\mathbf{A_3}$ (A), $\mathbf{A_3}$**.TFA** (B), 4-imidazolecarboxaldehyde $\mathbf{A_4}$ (C), the crystals obtained from a $\mathbf{A_4}$ 95:5 (v/v) TFA/H_2O solution (D), and the powder sample obtained from the sample in spectrum D dissolved in water and then lyophilized (E).

HA_2.2TFA, although the resolution at 30 kHz MAS in the ^{1}H NMR spectra was not enough to allow the elucidation of the chemical composition of the solids (Figure 4). This phenomenon is due to the superimposition of the signal corresponding to the proton bound to the *gem*-diol carbon (-C**H**$(OH)_2$) and the aromatic protons at δ^1H = 7−6 ppm (Figure 4). Furthermore, the presence of SAW environments observed for samples corresponding to spectra B and C (Figure 4) overlap with the resonance signal associated with the hydroxyl groups of the *gem*-diol and hemiacetal moieties in $\mathbf{H_1}$ and $\mathbf{H_1}$**.TFA**/$\mathbf{HA_1}$**.2TFA**, respectively. Then, the aldehyde form of compound $\mathbf{A_2}$ (25%) is observed at a proton chemical shift of 9.7 ppm with 75% of a mixture of *gem*-diol and hemiacetal structures. However, no evidence for the presence of the aldehyde form was found in the ^{13}C CP-MAS spectrum, in which only the profiles corresponding to the *gem*-diol ($\mathbf{H_2}$) and hemiacetal ($\mathbf{HA_2}$) forms were present. In addition, the ^{1}H MAS NMR spectrum of the sample containing only the *gem*-diol form ($\mathbf{H_2}$), as determined by ^{13}C CP-MAS experiments, shows that the aldehyde ($\mathbf{A_2}$) structures were also present in the same solid due to the interconversion of the *gem*-diol into the carbonyl form at the high MAS rate (Figure 4D).

3.3. HRMS Experiments. To complement the study, HRMS experiments were done for the solids studied in spectra B and C of Figure 1 dissolved in 50:50 (v/v) methanol/water, and the results are shown in Figure 5. For the crystals obtained from 95:5 (v/v) TFA/H_2O and 2-imidazolecarboxaldehyde ($\mathbf{A_1}$), the oxonium was the main ion (m/z = 111.056 82), which was generated after the loss of water from the corresponding parent hemiacetal (m/z = 129.066 62 (M+H) or 165.063 45 (M+Na)). Such hemiacetal resulted from the addition of methanol to the carbonyl group in 2-imidazolecarboxaldehyde (m/z = 97.040 37 (M+H)). Regarding the *gem*-diol ion, a relative abundance of only 0.7% was observed in methanol/water, and no higher m/z ions were present in the sample (Figure 5). Once again, the results obtained in HRMS experiments performed with the crystals obtained from 95:5 (v/v) TFA/H_2O and *N*-methyl-2-imidazolecarboxaldehyde dissolved in 50:50 (v/v) methanol/water were in line with the ss-NMR and X-ray analyses performed with 2-imidazolecarboxaldehyde and presented above, in which the presence of ions corresponding to the hemiacetal structure ($\mathbf{HA_2}$**.2TFA**) could not be demonstrated (Figures 1, 2, and S31). However, when the sample was dissolved in 20:60:20 (v/v) water/methanol/DMSO, it was possible to increase the relative content of the ions related to the *gem*-diol forms for 2-imidazolecarboxaldehyde ($\mathbf{H_1}$, m/z = 115.04996, 19.5%) and *N*-methyl-2-imidazolecarboxaldehyde ($\mathbf{H_2}$, m/z = 129.0673, 23%) (Figures S30 and S32).

To demonstrate that methanol altered the chemical composition of the solid sample, the neutral *gem*-diol form $\mathbf{H_1}$ (100%, according to ^{13}C CP-MAS results) was dissolved in deuterated methanol (CD_3OD). After this procedure, the contents of *gem*-diol and aldehyde were found to be 37% and 63%, respectively (Figure S3). When the solid sample studied containing both $\mathbf{H_1}$**.TFA** and $\mathbf{HA_1}$**.2TFA** molecules (Figure 1B) was dissolved in DMSO-d_6, the *gem*-diol ($\mathbf{H_1}$), aldehyde ($\mathbf{A_1}$), and hemiacetal ($\mathbf{HA_1}$) forms were 16%, 42%, and 42% (Figure S1), respectively, thus predicting that the *gem*-diol form would be significantly reduced prior to the HRMS study. In fact, the results obtained by HRMS performed in 20:60:20 (v/v) water/methanol/DMSO for $\mathbf{H_1}$ showed a relative abundance of only 19.5% for the *gem*-diol form (Figure S30).

3.4. Hydration Studies in 4- and 5-Imidazolecarboxaldehydes. To study the possibility of producing *gem*-diol moieties in other positions of the imidazole ring, the hydration of the carbonyl group in 4- and 5-imidazolecarboxaldehyde compounds was analyzed. The crystals obtained from 95:5 (v/v) TFA/H_2O with $\mathbf{A_3}$ and $\mathbf{A_4}$ showed that the structures corresponded to the carbonyl forms in both cases (Figure 2). In addition, the analysis of the remaining solid obtained from compound $\mathbf{A_4}$ indicated the presence of both the carbonyl and the carboxylic acid derivatives, as assessed by NMR (Figure 6 and Supporting Information). Although the solution-state NMR results for $\mathbf{A_{3-4}}$ showed that the *gem*-diol structure was present in 5% and 40% in 95:5 (v/v) D_2O/TFA (Table 1 and Figures S8−S11), the *gem*-diol forms detected by solution-state NMR experiments could not be isolated in the solid state (Figure 6). For instance, when the sample containing 4-formylimidazolium ($\mathbf{A_4}$**.TFA**) and 4-carboxy-imidazolium ($\mathbf{CA_4}$**.TFA**) trifluoroacetates was dissolved in D_2O, the *gem*-diol content was 38% (Figure S12). This value is close to the

DOI: 10.1021/acs.jpca.7b12390
J. Phys. Chem. A 2018, 122, 601−609

one obtained when $\mathbf{A_4}$ was treated with 95:5 (v/v) D_2O/TFA, together with 38% and 24% for the carboxyl and carbonyl derivatives, respectively (Table 1 and Figure S11). Moreover, when the same solid containing both **A_4.TFA** and **CA_4.TFA** was dissolved in DMSO-d_6, the *gem*-diol form was not observed (Figure S13).

Furthermore, the solid studied in spectrum D in Figure 6 shows that neutral $\mathbf{A_4}$ molecules (-**C**HO, $\delta^{13}C$ = 181.9 ppm) are still present in the crystalline samples and cannot be inferred from the solution-state NMR experiments. However, when the sample containing both $\mathbf{A_4}$ and **A_4.TFA** was treated with water, the sample became homogeneous, and only the protonated $\mathbf{A_4}$ molecules were observed (Figure 6E).

As for the position of the carbonyl group in the imidazole ring, our results showed a higher oxidative susceptibility when the aldehyde was at position 4 of the imidazole ring than in the case of 4-methyl-5-imidazolecarboxaldehyde. Thus, during the incubation with TFA, 4-imidazolecarboxaldehyde was oxidized to render the corresponding 4-carboxylic-imidazole acid due to the progression to the *gem*-diol form after the addition of water, which was higher than in the case of 4-methyl-5-imidazole-carboxaldehyde.

Likewise, a 2D solid-state $^1H-^{13}C$ HETCOR was performed to facilitate the analysis of the proton dimension and to clearly discriminate the corresponding hydrogen atoms of the carboxyl group of the $\mathbf{CA_4}$ in the mixture of compounds obtained in the incubation of $\mathbf{A_4}$ in TFA (Figure 7). The splitting observed in

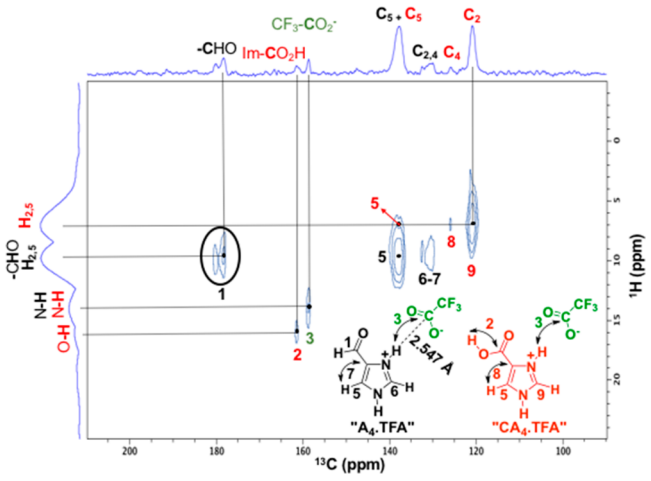

Figure 7. 2D $^1H-^{13}C$ HETCOR spectrum for the crystals obtained from the TFA solution with 4-imidazolecarboxaldehyde $\mathbf{A_4}$.

the carbon dimension for the carbonyl carbon at $\delta \approx 180$ ppm with its bound aldehyde hydrogen indicates the existence of a group of $\mathbf{A_4}$ molecules constituted by protonated and neutral species. Furthermore, two different kinds of protons can be easily assigned in the indirect dimension. These protons are associated with a long-range interaction with the carbon of the carboxylic acid present in TFA and 4-carboxy-imidazole molecules. The distance of such interaction, estimated through NMR analysis, was obtained from crystallography experiments performed with **A_4.TFA** and was found to be 2.547 Å ($F_3CCO_2\cdots$**H**-N-Im; Figure 7).

Finally, the hydration studies conducted on 2-, 4-, or 5-imidazolecarboxaldehydes indicated that the position of the carbonyl group was key to obtain the *gem*-diol function by treatment with TFA both in solution and in solid state. The $\mathbf{A_{3-4}}$ derivatives showed a lower degree of hydration of the aldehyde group than $\mathbf{A_1}$ and $\mathbf{A_2}$. However, because of the high reactivity of the aldehyde carbon toward water addition induced by TFA, both *gem*-diol and hemicetal forms could be isolated ($\mathbf{H_1}$, $\mathbf{HA_1}$, $\mathbf{H_2}$, and $\mathbf{HA_2}$). The single crystals of $\mathbf{A_{3-4}}$ showed only the presence of aldehyde groups, in contrast to the *gem*-diol and hemiacetal forms of $\mathbf{A_1}$ and $\mathbf{A_2}$, respectively (Figure 2). These differences are due to the specific electronic density of the imidazole ring positions; that is, one of the nitrogen atoms is mesomeric electron-donating (N_1), and the other one is electron-withdrawing (N_3).[39] Taking into account these results, it can be postulated that the lower reactivity of the aldehyde group in $\mathbf{A_3}$ toward the addition of water would explain why in copper, cadmium, zinc, and cobalt complexes the formyl group remains unhydrated.[21,40] The same results have been obtained for a complex of zinc(II) and $\mathbf{A_4}$.[23] An iron(III) complex was also reported with a new 4-imidazolecarboxaldehyde ligand in which the formyl group was not altered.[41] In contrast, the aldehyde group is hydrated to the *gem*-diol form in ruthenium-(III) complexes with 2-imidazolecarboxaldehyde ($\mathbf{A_1}$) molecules in the solution state.[22]

To demonstrate that the second position of the imidazole ring is particularly effective for the generation of *gem*-diol derivatives when the carbonyl group is present in this position, other aromatic compounds were analyzed (Table 1 and Supporting Information). For 2-thiophenecarboxaldehyde ($\mathbf{T_2}$) and ethyl 3-(5-formyl-2,4-dimethyl-1*H*-pyrrol-3-yl)-propanoate ($\mathbf{P_2}$), no evidence of hydration of the aldehyde group was observed even when 95:5 (v/v) D_2O/TFA was employed (Table 1 and Figure S18). In contrast, 4-methylthiazole-2-carboxaldehyde ($\mathbf{T_1}$) was completely hydrated in TFA, demonstrating that the electronic density is a crucial factor for the polarization of the carbonyl group and the addition of water in acidic medium (Table 1 and Figure S16).[39] Although 4-methylthiazole-2-carboxaldehyde ($\mathbf{T_1}$) was completely hydrated, as assessed by solution-state NMR experiments, the *gem*-diol form was not solid; therefore, crystallographic and ss-NMR analyses could not be performed. Ethyl 3-(5-formyl-2,4-dimethyl-1*H*-pyrrol-3-yl)propanoate dehyde ($\mathbf{P_2}$) was selected, because the absence of free positions in the aromatic ring prevents its decomposition by TFA. The X-ray and ss-NMR results for this compound are shown in the Supporting Information (Figures S27−S29).

4. CONCLUSIONS

This study assesses the generation and stability of the *gem*-diol forms in imidazole derivatives containing carbonyl groups. The hydration studies performed by solution- and solid-state NMR indicated that the position of the carbonyl group was essential to stabilize the *gem*-diol form or even to increase the reactivity to obtain hemiacetal forms in 2-formylimidazole compounds. The *gem*-diol or hemiacetal forms of $\mathbf{A_{1-2}}$ were obtained and studied by ss-NMR and crystallographic techniques. In addition, the corresponding carbonyl forms were observed in $\mathbf{A_{3-4}}$ derivatives under the same conditions under which $\mathbf{A_{1-2}}$ were completely hydrated. These results indicate that positions 4 and 5 of the imidazole ring did not effectively sense the electron-withdrawing character of the entire system upon protonation, as observed for 2-thiophenecarboxaldehyde ($\mathbf{T_2}$) and ethyl 3-(5-formyl-2,4-dimethyl-1*H*-pyrrol-3-yl)propanoate ($\mathbf{P_2}$).

Unlike pyridinecarboxaldehydes, the formyl groups in imidazolecarboxaldehydes do not incorporate water under

DOI: 10.1021/acs.jpca.7b12390
J. Phys. Chem. A 2018, 122, 601−609

neutral conditions. Instead, the *gem*-diol forms can be generated with the addition of TFA, which favors the nucleophilic addition of water. This phenomenon is possible due to the increase of the electron-withdrawing character of the imidazole ring upon protonation. Remarkably, our results indicated that, although TFA increased the *gem*-diol content, the position of the formyl group determines the possibility of obtaining the *gem*-diol solid structure, being the second position of the imidazole ring the only one that particularly senses the electron-withdrawing character. These differences are due to the specific electronic density of the imidazole ring positions, since the formyl group in 4-methyl-2-thiazolecarboxaldehyde ($\mathbf{T_1}$) was completely hydrated, whereas such group was not hydrated in 2-thiophenecarboxaldehyde ($\mathbf{T_2}$) and 3,5-dimethyl-4-carboxyethylpyrrole-2-carboxaldehyde ($\mathbf{P_2}$) when the same experimental conditions were employed.

■ ASSOCIATED CONTENT

Supporting Information

The Supporting Information is available free of charge on the ACS Publications website at DOI: 10.1021/acs.jpca.7b12390.

Crystallographic information for each compound: crystal data and structure refinement results, crystal structure with numbering and packing schemes, tables of fractional coordinates and equivalent isotropic displacement parameters of the non-H atoms, bond lengths and angles, atomic anisotropic displacement parameters, hydrogen atom positions and torsion angles. *Solution-state* NMR spectra for all the compounds studied in the present work (PDF)

X-ray crystallographic data (CIF)

Structural data of **H_1.TFA**, **HA_2.2TFA**, **A_3.TFA**, **A_4.TFA**, and **P_2** compounds were deposited as CIF files at the Cambridge Crystallographic Database (CCDC Nos. 1471036, 1471037, 1471039, 1471041, and 1471044) and can be downloaded freely from http://ccdc.cam.ac.uk.

■ AUTHOR INFORMATION

Corresponding Author

*Phone/Fax: +54-11-5287-4323. E-mail: lazarojm@ffyb.uba.ar and jmlazaromartinez@gmail.com.

ORCID

Gustavo Alberto Monti: 0000-0001-6531-798X

Juan Manuel Lázaro-Martínez: 0000-0002-7189-6874

Notes

The authors declare no competing financial interest.

■ ACKNOWLEDGMENTS

This work was performed with the financial support from ANPCYT (PICT 2012-0151, PICT 2014-1295, and PICT 2016-1723), Univ. de Buenos Aires (UBACyT 2017-2019/22BA), CONICET (PIP 2014-2016/130), and SeCyT Univ. Nacional de Córdoba. A.F.C. and A.J.B. are grateful for their doctoral and undergraduate fellowships granted by Univ. de Buenos Aires, respectively.

■ REFERENCES

(1) Woodruff, D. N.; Winpenny, R. E. P.; Layfield, R. A. Lanthanide Single-Molecule Magnets. *Chem. Rev.* **2013**, *113*, 5110−5148.

(2) Liu, J.-L.; Lin, W.-Q.; Chen, Y.-C.; Gómez-Coca, S.; Aravena, D.; Ruiz, E.; Leng, J.-D.; Tong, M.-L. Cu(II)-Gd(III) Cryogenic Magnetic Refrigerants and Cu8Dy9 Single-Molecule Magnet Generated by in Situ Reactions of Picolinaldehyde and Acetylpyridine: Experimental and Theoretical Study. *Chem. - Eur. J.* **2013**, *19*, 17567−17577.

(3) Llano-Tomé, F.; Bazán, B.; Karmele Urtiaga, M.; Barandika, G.; Fidalgo-Marijuan, A.; Fernández De Luis, R.; Arriortua, M. I. Water-Induced Phase Transformation of a CuII-Coordination Framework with Pyridine-2,5- Dicarboxylate and Di-2-Pyridyl Ketone: Synchrotron Radiation Analysis. *CrystEngComm* **2015**, *17*, 6346−6354.

(4) Tasiopoulos, A. J.; Perlepes, S. P. Diol-Type Ligands as Central "players" in the Chemistry of High-Spin Molecules and Single-Molecule Magnets. *Dalt. Trans.* **2008**, *41*, 5537−5555.

(5) Stamatatos, T. C.; Nastopoulos, V.; Tasiopoulos, A. J.; Moushi, E. E.; Wernsdorfer, W.; Christou, G.; Perlepes, S. P. High Nuclearity Single-Molecule Magnets: A Mixed-Valence Mn Cluster Containing the Di-2-Pyridylketone Diolate Dianion High Nuclearity Single-Molecule Magnets: A Mixed-Valence Mn26 Cluster Containing the Di-2-Pyridylketone Diolate Dianion. *Inorg. Chem.* **2008**, *47*, 10081−10089.

(6) Savva, M.; Skordi, K.; Fournet, A. D.; Thuijs, A. E.; Christou, G.; Perlepes, S. P.; Papatriantafyllopoulou, C.; Tasiopoulos, A. J. Heterometallic MnIII4Ln2 (Ln = Dy, Gd, Tb) Cross-Shaped Clusters and Their Homometallic MnIII4MnII2 Analogues. *Inorg. Chem.* **2017**, *56*, 5657−5668.

(7) Wang, H.-S.; Yang, F.-J.; Long, Q.-Q.; Huang, Z.-Y.; Chen, W.; Pan, Z.-Q. Syntheses, Crystal Structures, and Magnetic Properties of a Family of Heterometallic Octanuclear [Cu6Ln2] (Ln = Dy(III), Tb(III), Ho(III), Er(III), and Gd(III)) Complexes. *New J. Chem.* **2017**, *41*, 5884−5892.

(8) Giannopoulos, D. P.; Cunha-Silva, L.; Ballesteros-Garrido, R.; Ballesteros, R.; Abarca, B.; Escuer, A.; Stamatatos, T. C. New Structural Motifs in Mn Cluster Chemistry from the Ketone/gem-Diol and Bis(gem-Diol) Forms of 2,6-Di-(2-Pyridylcarbonyl)pyridine: {MnII4MnIII2} and {MnII4MnIII6} Complexes. *RSC Adv.* **2016**, *6*, 105969−105979.

(9) Bravo-García, L.; Barandika, G.; Bazán, B.; Urtiaga, M. K.; Arriortua, M. I. Thermal Stability of Ionic Nets with CuII Ions Coordinated to Di-2-Pyridyl Ketone: Reversible Crystal-to-Crystal Phase Transformation. *Polyhedron* **2015**, *92*, 117−123.

(10) Efthymiou, C. G.; Raptopoulou, C. P.; Psycharis, V.; Tasiopoulos, A. J.; Escuer, A.; Perlepes, S. P.; Papatriantafyllopoulou, C. Copper(II)/di-2-Pyridyl Ketone Chemistry: A Triangular Cluster Displaying Antisymmetric Exchange versus an 1D Coordination Polymer. *Polyhedron* **2013**, *64*, 30−37.

(11) González Mantero, D.; Altaf, M.; Neels, A.; Stoeckli-Evans, H. Pyridin-4-Ylmethanediol: The Hydrated Form of Isonicotinaldehyde. *Acta Crystallogr., Sect. E: Struct. Rep. Online* **2006**, *62*, o5204−o5206.

(12) Melaiye, A.; Sun, Z.; Hindi, K.; Milsted, A.; Ely, D.; Reneker, D. H.; Tessier, C. A.; Youngs, W. J. Silver(I)−Imidazole Cyclophane Gem-Diol Complexes Encapsulated by Electrospun Tecophilic Nanofibers: Formation of Nanosilver Particles and Antimicrobial Activity. *J. Am. Chem. Soc.* **2005**, *127*, 2285−2291.

(13) Wang, W.; Spingler, B.; Alberto, R. Reactivity of 2-Pyridine-Aldehyde and 2-Acetyl-Pyridine Coordinated to [Re(CO)3]+ with Alcohols and Amines: Metal Mediated Schiff Base Formation and Dimerization. *Inorg. Chim. Acta* **2003**, *355*, 386−393.

(14) Yang, G.; Tong, M. L.; Chen, X. M.; Ng, S. W. Bis(di-2-Pyridylmethanediol-N, O,N')- copper(II) Diperchlorate. *Acta Crystallogr., Sect. C: Cryst. Struct. Commun.* **1998**, *54*, 732−734.

(15) Bock, H.; Van, T. T. H.; Schödel, H.; Dienelt, R. Structural Changes of Di(2-Pyridyl) Ketone on Single and Twofold Protonation. *Eur. J. Org. Chem.* **1998**, *1998*, 585−592.

(16) Wang, S. L.; Richardson, J. W.; Briggs, S. J.; Jacobson, R. A.; Jensen, W. P. Stabilization of a Hydrated Ketone by Metal Complexation. The Crystal and Molecular Structures of Bis-2,2', N,N'-Bipyridyl Ketone-Hydrate Nickel(II) Sulfate, Copper(II) Chloride and Copper(II) Nitrate. *Inorg. Chim. Acta* **1986**, *111*, 67−72.

(17) Zhang, X.; Bruning, J. B.; George, J. H.; Abell, A. D. A Mechanistic Study on the Inhibition of α-Chymotrypsin by a Macrocyclic Peptidomimetic Aldehyde. *Org. Biomol. Chem.* **2016**, *14*, 6970−6978.

(18) Oslaj, M.; Cluzeau, J.; Orkic, D.; Kopitar, G.; Mrak, P.; Casar, Z. A Highly Productive, Whole-Cell DERA Chemoenzymatic Process for Production of Key Lactonized Side-Chain Intermediates in Statin Synthesis. *PLoS One* **2013**, *8*, e62250.
(19) Crespi, A. F.; Vega, D.; Chattah, A. K.; Monti, G. A.; Buldain, G. Y.; Lázaro-Martínez, J. M. Gem-Diol and Hemiacetal Forms in Formylpyridine and Vitamin-B6-Related Compounds: Solid-State NMR and Single-Crystal X-Ray Diffraction Studies. *J. Phys. Chem. A* **2016**, *120*, 7778−7785.
(20) Lázaro Martínez, J. M.; Romasanta, P. N.; Chattah, A. K.; Buldain, G. Y. NMR Characterization of Hydrate and Aldehyde Forms of Imidazole-2-Carboxaldehyde and Derivatives. *J. Org. Chem.* **2010**, *75*, 3208−3213.
(21) Barszcz, B. Coordination Properties of Didentate N, O Heterocyclic Alcohols and Aldehydes towards Cu(II), Co(II), Zn(II) and Cd(II) Ions in the Solid State and Aqueous Solution. *Coord. Chem. Rev.* **2005**, *249*, 2259−2276.
(22) Elliott, M. G.; Shepherd, R. E. Pentaammineruthenium(II/III) Imidazole and Imidazolate Complexes of 2-Carboxylatoimidazole and 2-Imidazolecarboxaldehyde. *Inorg. Chem.* **1987**, *26*, 2067−2073.
(23) Won, M. S.; Lee, Y. H.; Rukmini, E.; Harrowfield, J. M.; Kim, Y. Aldehyde Coordination in Template Reactions: Crystal Structure of a Possible Reaction Intermediate. *Inorg. Chem. Commun.* **2013**, *38*, 156−159.
(24) Seredyuk, M.; Gaspar, A. B.; Kusz, J.; Gütlich, P. Mononuclear Complexes of Iron(II) Based on Symmetrical Tripodand Ligands: Novel Parent Systems for the Development of New Spin Crossover Metallomesogens. *Z. Anorg. Allg. Chem.* **2011**, *637*, 965−976.
(25) Liao, Y. Te; Dutta, S.; Chien, C. H.; Hu, C. C.; Shieh, F. K.; Lin, C. H.; Wu, K. C. W. Synthesis of Mixed-Ligand Zeolitic Imidazolate Framework (ZIF-8−90) for CO2 Adsorption. *J. Inorg. Organomet. Polym. Mater.* **2015**, *25*, 251−258.
(26) Brewer, C.; Brewer, G.; Butcher, R. J.; Carpenter, E. E.; Cuenca, L.; Noll, B. C.; Scheidt, W. R.; Viragh, C.; Zavalij, P. Y.; Zielaski, D. Synthesis and Characterization of manganese(II) and iron(III) d5 Tripodal Imidazole Complexes. Effect of Oxidation State, Protonation State and Ligand Conformation on Coordination Number and Spin State. *Dalton Trans.* **2006**, *8*, 1009−1019.
(27) Qin, L.-F.; Pang, C.-Y.; Han, W.-K.; Zhang, F.-L.; Tian, L.; Gu, Z.-G.; Ren, X.; Li, Z. Optical Recognition of Alkyl Nitrile by a Homochiral iron(II) Spin Crossover Host. *CrystEngComm* **2015**, *17*, 7956−7963.
(28) Cruz-Enriquez, A.; Baez-Castro, A.; Hopfl, H.; Parra-Hake, M.; Campos-Gaxiola, J. J. Tetrakis(u-Acetato-k2O: O')-bis[(3-Pyridine-carboxaldehyde-kN')]-dicopper(II)(Cu—Cu). *Acta Crystallogr., Sect. E: Struct. Rep. Online* **2012**, *68*, m1339−m1340.
(29) Efthymiou, C. G.; Papatriantafyllopoulou, C.; Aromi, G.; Teat, S. J.; Christou, G.; Perlepes, S. P. A NiII Cubane with a Ligand Derived from a Unique Metal Ion-Promoted, Crossed-Aldol Reaction of Acetone with Di-2-Pyridyl Ketone. *Polyhedron* **2011**, *30*, 3022−3025.
(30) Krzemińska, A.; Moliner, V.; Świderek, K. Dynamic and Electrostatic Effects on the Reaction Catalyzed by HIV-1 Protease. *J. Am. Chem. Soc.* **2016**, *138*, 16283−16298.
(31) Das, A.; Mahale, S.; Prashar, V.; Bihani, S.; Ferrer, J. L.; Hosur, M. V. X-Ray Snapshot of HIV-1 Protease in Action: Observation of Tetrahedral Intermediate and Short Ionic Hydrogen Bond SIHB with Catalytic Aspartate. *J. Am. Chem. Soc.* **2010**, *132*, 6366−6373.
(32) Davies, J. L. A Synthesis of 2,6-Diacetyldeuterioporphyrin II Dimethyl Ester. *J. Chem. Soc. C* **1968**, 1392−1396.
(33) Fung, B. M.; Khitrin, A. K.; Ermolaev, K. An Improved Broadband Decoupling Sequence for Liquid Crystals and Solids. *J. Magn. Reson.* **2000**, *142*, 97−101.
(34) van Rossum, B.-J.; Förster, H.; de Groot, H. J. M. High-Field and High-Speed CP-MAS 13C NMR Heteronuclear Dipolar-Correlation Spectroscopy of Solids with Frequency-Switched Lee−Goldburg Homonuclear Decoupling. *J. Magn. Reson.* **1997**, *124*, 516−519.
(35) Sheldrick, G. M. Phase Annealing in SHELX-90: Direct Methods for Larger Structures. *Acta Crystallogr., Sect. A: Found. Crystallogr.* **1990**, *46*, 467−473.
(36) Sheldrick, G. M. A Short History of SHELX. *Acta Crystallogr., Sect. A: Found. Crystallogr.* **2008**, *64*, 112−122.
(37) Turov, V. V.; Gun'ko, V. M.; Zarko, V. I.; Leboda, R.; Jablonski, M.; Gorzelak, M.; Jagiello-Wojtowicz, E. Weakly and Strongly Associated Nonfreezable Water Bound in Bones. *Colloids Surf., B* **2006**, *48*, 167−175.
(38) Gun'ko, V. M.; Savina, I. N.; Mikhalovsky, S. V. Cryogels: Morphological, Structural and Adsorption Characterisation. *Adv. Colloid Interface Sci.* **2013**, *187−188*, 1−46.
(39) Berezin, M. Y.; Kao, J.; Achilefu, S. PH-Dependent Optical Properties of Synthetic Fluorescent Imidazoles. *Chem. - Eur. J.* **2009**, *15* (14), 3560−3566.
(40) Barszcz, B.; Hodorowicz, S. A.; Stadnicka, K.; Jabłońska-Wawrzycka, A. A Comparison of the Coordination Geometries of Some 4-Methylimidazole-5-Carbaldehyde Complexes with Zn(II), Cd(II) and Co(II) Ions in the Solid State and Aqueous Solution. *Polyhedron* **2005**, *24*, 627−637.
(41) Li, J.; Molenda, M. A.; Biros, S. M.; Staples, R. J.; Chavez, F. A. Assembly of a Mononuclear Ferrous Site Using a Bulky Aldehyde-Imidazole Ligand. Inorganica Chim. *Inorg. Chim. Acta* **2017**, *464*, 152−156.

DOI: 10.1021/acs.jpca.7b12390
J. Phys. Chem. A 2018, 122, 601−609